Nanoscale

Accepted Manuscript

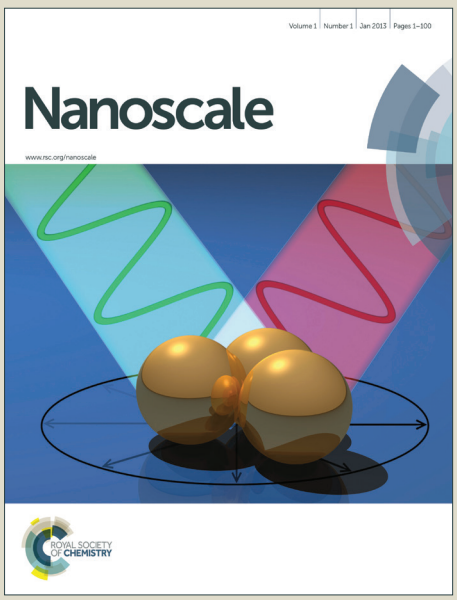

ROYAL SOCIETY OF CHEMISTRY

www.rsc.org/nanoscale

Cite this: DOI: 10.1039/c0xx00000x

www.rsc.org/xxxxxx

ARTICLE TYPE

An efficient one-step condensation and activation strategy to synthesize porous carbons with optimal micropore sizes for highly selective CO_2 adsorption

Jiacheng Wang,* and Qian Liu*

Received (in XXX, XXX) Xth XXXXXXXXX 20XX, Accepted Xth XXXXXXXXX 20XX
DOI: 10.1039/b000000x

A series of microporous carbons (MPCs) were successfully prepared by an efficient one-step condensation and activation strategy using commercial available dialdehyde and diamine as carbon sources. The resulting MPCs have large surface areas of up to 1881 m^2/g, micropore volumes (up to 0.78 cm^3/g), and narrow micropore size distributions (0.7-1.1 nm). The CO_2 uptakes of the MPCs prepared at high temperatures (700-750 °C) are higher than those prepared at mild conditions (600-650 °C), because the former samples possess the optimal micropore sizes (0.7-0.8 nm), highly suitable for CO_2 capture due to enhanced adsorbate-adsorbent interaction. At 1 bar, MPC-750 prepared at 750 °C demonstrates the best CO_2 capture performance and can efficiently adsorb CO_2 molecules of 2.86 mmol/g and 4.92 mmol/g, at 25 and 0 °C, respectively. Particularly, the MPCs with optimal micropore sizes (0.7-0.8 nm) have extremely high CO_2/N_2 adsorption ratios (47 and 52 at 25 and 0 °C, respectively) at 1 bar and initial CO_2/N_2 adsorption selectivity of up to 81 and 119 at 25 °C and 0 °C, respectively, which are far superior to the previously reported values for various porous solids. These excellent data combined with good adsorption capacities and efficient regeneration/recyclability, make these carbons amongst the most promising sorbents reported so far for selective CO_2 adsorption in practical applications.

Introduction

In view of the predicted detrimental effects (*e. g.*, global climate warming) of CO_2 emission, there is growing interest in developing new materials and technologies for CO_2 adsorption and separation. At present, well-developed chemical processes based on adsorption and regeneration are employed for CO_2 separation on large scale using various aqueous amine-ammonia solutions in industry.[1] However these processes are not only corrosive but also highly energy-costing because of the energy penalty necessary for regenerating aqueous amine-based solutions. Compared to the conventional chemical adsorption processes, the use of porous solid materials as sorbents based on the physisorption allows conveniently reversible processes to capture and release CO_2, and thus it is a greener and more cost-efficient method. To date, numerous porous solids (*e. g.*, porous carbons, zeolites, mesoporous silica, metal-organic frameworks (MOFs), and porous organic polymers) have been developed for CO_2 capture and separation.[2-14]

Among these porous solids, porous carbons are considered to be one of the promising, sustainable for capturing CO_2 due to their light weight, low cost, fast adsorption kinetics, large surface area, and high chemical and thermal stability.[15-20] Lots of studies were performed to prepare various porous carbons and investigate their CO_2 uptake capacities. For example, by direct pyrolysis of porous imine-linked polymers,[21] self-assembled poly(benzoxazine-co-resol),[10] and resorcinol-formaldehyde resin,[11] various nitrogen-doped porous carbons were formed, showing CO_2 adsorption capacities of 2.7-5.5 mmol/g at 0 °C and 1 bar. Porous carbons, synthesized by the template method in which the combination of nanocasting and etching offing the templates is needed, demonstrated the CO_2 adsorption capacities of 2.3-5 mmol/g at ambient temperature and pressure.[22] Recently, Su and co-workers reported the modification of porous carbon monoliths by doping carbon nanotubes, and the resulting composite has a CO_2 uptake of 3.5 mmol/g at 1 bar and 25 °C.[23] Although these porous carbons have been moderated to good CO_2 uptakes, they demonstrate the poor CO_2/N_2 adsorption selectivity, generally lower than 15. Because half of the anthropogenic CO_2 emission is ascribed to the combustion of fossil fuel in power plants, in which large amount of flue gases composed of 75% N_2 and 15% CO_2 is let out,[24] porous carbons with high adsorption ratio and adsorption selectivity of CO_2/N_2 are urgently on demand to capture and separate CO_2 from these flue gases containing high concentration of N_2.

At present, the effective chemical activation and nitrogen functionalization of carbonaceous materials are flexibly performed to obtain porous carbons with variable porosity, pore size distribution, and surface basic functional groups, thus leading to different CO_2 uptake capacities and CO_2/N_2 adsorption selectivity. Recently biomass-based carbonaceous materials, polymers, templated porous carbons, and carbide-derived carbons were activated by KOH to create large porosity in final porous

carbons. These carbons show good CO_2 adsorption capacities, but they have poor CO_2/N_2 adsorption selectivity lower than 17.[22, 25-29] The activation of graphene-filled polypyrrole or polyaniline by KOH led to a similar CO_2/N_2 adsorption ratio (<17) as the un-doped ones.[30-31] Moreover, the CO_2 uptakes of these activated carbons evidently decrease as the increment of the activation temperature because of pore widening. Especially it has been confirmed that pores smaller than 0.8 nm contribute to most of the CO_2 uptake because of the enhanced CO_2-adsorbent interactions.[32-34] Thus we expect to prepare novel porous carbons possessing optimized pore size of 0.8 nm with enhanced CO_2 adsorption capacity, and very high CO_2/N_2 adsorption ratio and initial adsorption selectivity.

Recently, we reported the activation of porous imine-linked polymer with KOH to form nitrogen-incorporated porous carbons with very high surface areas of up to 3100 m^2/g,[35] which have CO_2 uptakes of up to 5.3 mmol/g at 1 bar and 0 °C. And the calculated initial CO_2/N_2 adsorption selectivity up to 23 and adsorption ratio of 6.6 at ambient pressure were obtained, which are better than most of the previously reported values. For practical applications in CO_2 adsorption and separation from the flue gases containing 75% N_2 and 15% CO_2, the adsorption ratios and initial adsorption selectivity of CO_2/N_2 for these porous carbons should be improved greatly. Furthermore these imine-linked polymers using multialdehydes and multiamines as monomers were prepared using large amount of high boiling point toxic organic solvents,[21, 36-38] and therefore the synthesis processes are not environmentally friendly.

In this paper, we develop an efficient one-pot condensation and activation strategy to synthesize microporous carbons (MPCs) using commercial available *m*-phenylenediamine and terephthalaldehyde as carbon sources, in which the additional step of preparing porous polymer in toxic organic solvents is avoided. Thus the present process for forming MPCs is very environmentally friendly and sustainable. The resulting MPCs have high surface areas, large micropore volumes, and narrow micropore size distributions as well as small amount of nitrogen doping depending on the activation temperatures (600-750 °C). It is worth noting that the samples prepared at high temperatures (700-750 °C) demonstrate smaller pore systems (0.7-0.8 nm) than those synthesized at relatively low temperatures (600-650 °C). The resulting MPCs have not only good CO_2 uptake capacities, but also extremely high CO_2/N_2 adsorption ratio (47-52) at 1 bar and initial adsorption selectivity (81-119). Therefore these MPCs have great potentials in CO_2 adsorption and separation from the flue gases of the fossil-fuel-fired power plants.

Experimental

Material synthesis

All reagents (*m*-phenylenediamine, terephthalaldehyde, potassium hydroxide (KOH), and concentrated HCl) were purchased from commercial sources (Sigma-Aldrich) without purification before use. Deionized water was used in all experiments.

The aromatic ditopic amine and aldehyde, *m*-phenylenediamine and terephthalaldehyde, are simple organic small molecules used as carbon sources in the present research. The mixture of amine and aldehyde (1:1 molar ratio) were added into KOH pellets with KOH/(amine+aldehyde) mass ratio of 3/2. Then the mixture was ground manually in a mortar with a pestle to crush KOH pellets for 20 min, resulting in thoroughly homogeneous mixture powder. This mixture was then placed into an alumina combustion boat and calcinated in a tubular furnace at the expected temperature for 1 h (ramp rate: 3 ºC/min) under an argon flow. After cooling to room temperature, the sample was thoroughly washed several times with 10 wt% HCl to remove inorganic salts, large amount of distilled water until neutral pH, and finally dried at 80 ºC overnight in an oven. The final carbons were named as MPC-T, where MPC is the abbreviation of microporous carbon and T is the activation temperature in ºC.

Material characterization

Nitrogen adsorption isotherms were collected at -196 ^oC using a Quantachrome Autosorb 1C apparatus. Prior to the gas adsorption measurement, the samples were degassed in vacuum at 150 ^oC overnight. Specific surface areas were calculated using the Brunauer-Emmett-Teller (BET) equation (p/p_0 = 0.05-0.20). The total pore volume was determined at relative pressure p/p_0 = 0.98. The pore size distribution was estimated according to the quenched solid density functional theory (QSDFT) method based on the equilibrium model for slit pores using the Autosorb 1.56 software from Quantachrome. The micropore volume and surface area were obtained *via* the t-plot analysis.

Nitrogen adsorption measurements at 0 or 25 ^oC and up to 1 bar were carried out using a Quantachrome Autosorb-1 instrument. Transmission electron microscopy (TEM) investigations were performed using a 200 kV JEOL 2010CX TEM instrument. SEM images were recorded using a JEOL JXA-8100 scanning electron analyzer. Powder X-ray diffraction (XRD) analysis was performed using a Rigaku D/MAX-λ B instrument with Cu $K\alpha_1$ radiation (40 kV, 60 mA). Fourier-transform infrared (FT-IR) spectroscopic investigation was carried out on a Nicolet FT-IR 205 spectrometer. Elemental analysis was carried out using a CHN elemental analyzer (Model 2400, Perkin-Elmer, Norwalk, CT). Thermal analysis (TGA) was performed using a Netzsch STA-449/C instrument. X-ray photoelectron spectra were recorded on a Kratos Axis Ultra DLD spectrometer employing a monochromatic Al KR X-ray source (75-150W) and analyzer pass energy of 160 eV (for survey scans) or 40 eV (for detailed scans).

CO_2 capture measurements

The CO_2 adsorption measurements were carried out using a Quantachrome Autosorb-1 instrument at 0 or 25 ^oC in low pressure range of up to 1 bar. Before the measurement the samples were degassed at 150 ^oC in vacuum for 24 h to remove any moisture and CO_2 molecules adsorbed in the pores. After the sample was cooled down to 0 or 25 °C, the CO_2 supplied was introduced into the system. To investigate the recyclability of MPCs for CO_2 capture, the used porous carbon was regenerated by evacuating at 150 °C for 1 h in vacuum and then re-used in CO_2 adsorption test.

Results and discussion

Fig. 1 (a) Schematic illustration of preparing MPCs from diamine and dialdehyde, and (b) reaction equation showing the condensation between terephthalaldehyde and *m*-phenylenediamine to form imine-based polymer with water as only by-product.

As presented in **Fig. 1a**, the colour of the mixture changes yellow when grinding the mixture of KOH, diamine, and dialdehyde in a mortar with a pestle at room temperature, which indicates the formation of the imine bonds (C=N) *via* the combination of the aldehyde and amine groups.[36] This reaction procedure happens based on the Schiff base condensation of the aldehyde and amine groups, which can proceed under ambient conditions in the absence of any catalyst with only water emission (**Fig. 1b**).[39] In comparison, porous imine-linked polymer was prepared in large amount of toxic organic solvents.[21, 36-38] The formation of the imine functional groups in the mixture obtained by grinding *m*-phenylenediamine and terephthalaldehyde was confirmed by the FT-IR characteristic spectrum. An evident imine stretch (C=N) is found at ~1626 cm^{-1} (**Fig. 2**), revealing the presence of the imine bands in the mixture, although a sharp band at *ca*. 1687 cm^{-1} due to the unreacted aldehydes is present.[36]

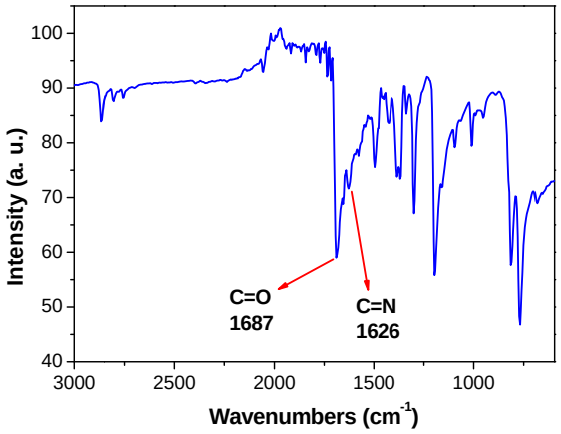

Fig. 2 FT-IR spectrum of the mixture of *m*-phenylenediamine and terephthalaldehyde obtained by grinding.

The thermal analysis of the ground mixture without KOH performed in nitrogen atmosphere shows the residual mass is *ca*. 55% at 600 °C (**Fig. 3**). This carbon yield is similar to that (50.1%) for the direct pyrolysis of porous imine-linked polymer prepared by the condensation of *m*-phenylenediamine and terephthalaldehyde in an organic solvent,[21] implying the present physical mixing strategy combined with pyrolysis also can obtain a good carbon yield. As shown in **Fig. 3**, there is a continual mass loss below 400 °C with several corresponding peaks in the DTG curve, which can be ascribed to the condensation of the unreacted aldehyde and amine groups as well as the evaporation of both the adsorbed moisture and water formed. In contrast, no evident mass change at between 150 and 400 °C was observed in the TG curve of porous imine-linked polymer.[37] This comparison further confirms that the unreacted amine and aldehyde groups in the grounded mixture can condense during the heat treatment. A strong exothermal peak at *ca*. 430 °C is the result of carbonizing the resultant polymer, which matches well with the previous study.[36-37] However the resulting carbon by directly heating the ground mixture at 700 °C has hardly any porosity confirmed by the nitrogen sorption measurement at -196 °C, and shows a surface area of only 7 m^2/g (**Fig. S1**). This low surface area, well in consistence with the external surface area determined by the α_s-plot technique,[40] is derived from the inter-particle voids, and there are no any framework-confined pores. This nonporous carbon with such low surface area is not appropriately utilized in various fields, such as gas adsorption and storage.[41]

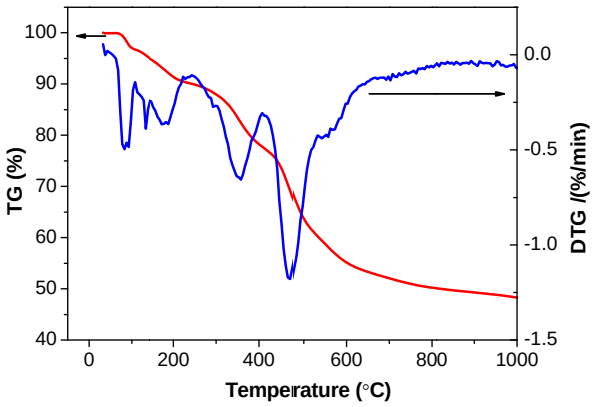

Fig. 3 TG-DTG curves of the ground mixture of *m*-phenylenediamine and terephthalaldehyde in an argon flow. At 800 °C, the residual mass is ~50 wt%.

To efficiently improve the surface area of final carbons, a one-pot condensation and activation strategy was adopted by directly adding KOH pellets as the activation reagent into the mixture of *m*-phenylenediamine and terephthalaldehyde when grinding, as shown in **Fig. 1**. The subsequent heat-treatment at 600-750 °C of the finely ground powder containing KOH not only promotes the condensation of the unreacted amine and aldehyde groups but also chemically activates the resulting polymer in one-step.[42] After washing using HCl aqueous solution to remove any inorganic impurities, porous carbons with high surface areas and large pore volumes were obtained. Obviously our one-step strategy, combining the polymerization and chemical activation to prepare porous carbons using small organic molecules, can avoid the usage of large amount of toxic organic solvents and, therefore, is economic and environmentally friendly.

During KOH activation process, the carbon combustion happens as the stoichoimetrical solid-solid/solid-liquid reaction,[43] shown in the equation $6KOH + 2C \rightarrow 2K + 3H_2 + 2K_2CO_3$. Thus the yields of porous carbons by KOH activation are evidently lower than that obtained by direct pyrolysis. As shown in Table 1, with higher activation temperatures the yields of porous carbons are lowered. The yields of the resulting porous carbons greatly decreased from 31 wt% for PC-600 to 14 wt% for PC-750 respectively (Table 1), all of which are lower than ~50 wt% obtained at 800 °C according to the thermal analysis. These

results indicate that more carbon was consumed during the activation as the increase of the activation temperature.

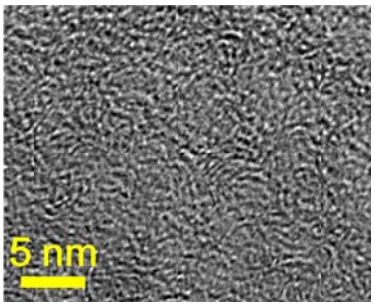

Fig. 4 High-resolution TEM (HRTEM) images of MPC-750.

The powder X-ray diffraction (XRD) patterns of the MPCs prepared at various temperatures are provided in **Fig. S2**. These patterns show two very broad features centred at ~20° and 44°, which are ascribed to the (002) and (100) diffractions, respectively. The broadening and low intensity of the bands indicate a very low degree of graphitic structure in these carbons. Also no diffractions due to any potassium compounds are observed, confirming the complete removal of potassium impurities by acid washing. Moreover, the high-resolution TEM (HRTEM) image exhibits that the porosity of these carbons is made up of randomly distributed micropores, as shown in **Fig. 4**. And the absence of long-range order in these carbons is well in consistence with the XRD analysis.

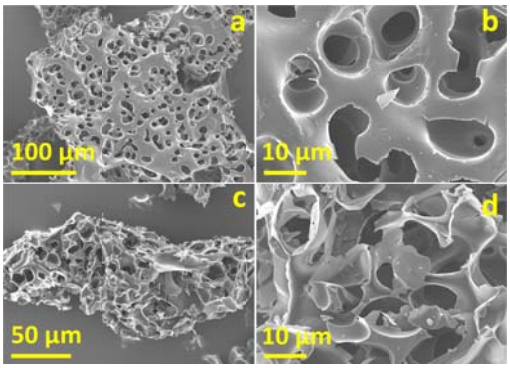

Fig. 5 SEM images of (a, b) MPC-650 and (c, d) MPC-750, indicating the existence of smooth large macropores.

The particle morphology of the MPCs is observed by the scanning electron microscopy (SEM). As presented in **Fig. 5**, all resulting carbon particles possess many large voids with pore size of over 10 µm, which have smooth surfaces. The formation of the macropores results from the gas bubble production during the activation at high temperatures. The sample MPC-650 prepared at low temperature (650 °C) owns relatively regular macropores which changed irregular and were partly collapsed in PC-750 prepared at high temperature (750 °C). At the same time, MPC-750 evidently has a thinner pore wall of macropores than MPC-650. These results are consistent with the trend of the carbon yields decreasing as the increment of the activation temperature. This phenomenon can be explained that at the activation temperature over 700 °C, the as-formed K_2CO_3 starts to decompose into CO_2 and K_2O.[44] Then CO_2 reacts with more carbon through the gasification of carbon, namely the physical activation, thus providing the lower carbon yields and leading to the thinner pore walls. The collaborative effects of the chemical activation, physical activation, and metal potassium intercalation lead to the high microporosity for final MPCs.[42]

Table 1. The yields and textural properties of various MPCs.

Sample	Yield (%)	S_{BET}/ $m^2 g^{-1}$	V_p[a]/ $cm^3 g^{-1}$	S_{micro}[b]/ $m^2 g^{-1}$	V_{micro}[b]/ $cm^3 g^{-1}$	D_{pore}[c]/ nm
MPC-600	31	1475	0.67	1422	0.62	1.1
MPC-650	22	1431	0.65	1391	0.61	1.0
MPC-700	19	1643	0.73	1592	0.68	0.7
MPC-750	14	1881	0.85	1811	0.78	0.8

[a] Total pore volume at $p/p_0 = 0.98$. [b] Micropore surface area and volume determined by the t-plot method. [c] Maxima of the pore size distribution calculated by the QSDFT method.

The presence of high microporosity in these MPCs is confirmed by the nitrogen adsorption measurements performed at -196 °C. The nitrogen adsorption isotherms and pore size distributions are shown in **Fig. 6a** and **6b**, respectively. The textural properties are collected in **Table 1**. All the adsorption isotherms for the resulting MPCs show a sharp rounded knee in the relative pressure (P/P_0) of 0.10-0.25. These isotherms are type I typical of microporous materials. The nitrogen uptakes for the samples prepared at high temperature are evidently larger than those obtained for the low-temperature activated samples, indicating the formation of the increasing porosity. Indeed, the samples prepared at 600 and 650 °C have similar surface areas (~1400 m^2/g) and pore volumes (0.65-0.67 cm^3/g), while the surface areas and pore volumes increase to 1643 m^2/g and 0.73 cm^3/g for PC-700, and then 1881 m^2/g and 0.85 cm^3/g for PC-750, respectively (**Table 1**). Moreover over 90% of the surface areas and pore volumes of these carbons are ascribed to those of micropores in all samples. The micropore sizes could be confirmed by the QSDFT pore size distributions shown in Fig. 6b. All activated carbons have a well-defined pore system in the micropore range. There are no any mesopores found in these porous carbons. The maximum of the pore size is 1.1 nm for MPC-600, and 1.0 nm for MPC-650, while MPC-700 and MPC-750 prepared at higher temperature demonstrate a smaller pore system (0.7-0.8 nm), possibly because of pore shrinking under high-temperature heat treatment. In contrast, porous carbons prepared by direct activation of polymer and biomass-based chars with high amounts of KOH (KOH/precursor mass ratio: 4/1-6/1) have increased pore sizes as the activation temperature and even a mesopore system is observed for the samples prepared at higher activation temperatures over 750 °C.[26, 29, 45] Therefore, these porous carbons prepared at high temperature demonstrate an evident loss of H_2 or CO_2 uptakes because of pore widening compared to those obtained at lower temperature.[26, 29, 45] Gogotsi and co-workers confirmed that pores smaller than 0.8 nm contribute most of the CO_2 uptake.[32] It is believed that the pores smaller than 0.8 nm are very effective for strengthening CO_2-adsorbent interactions.[33-34] Therefore it can be inferred that the high-temperature activated MPCs have excellent CO_2 adsorption capacities compared to those obtained at relatively low temperatures. The results also indicate that the present one-step condensation and activation strategy is highly efficient for controlling the micropore sizes of the final carbons especially at high temperatures.

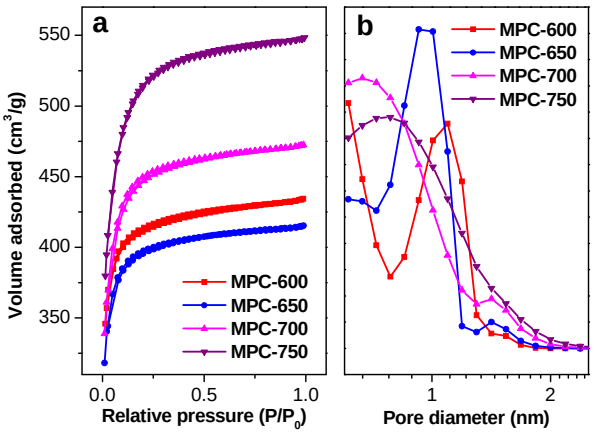

Fig. 6 Nitrogen adsorption isotherms (a) and QSDFT pore size distribution curves of various MPCs.

The chemical compositions of the resulting MPCs determined by CNH elemental analysis are illustrated in **Table 2**. All MPCs contain variable nitrogen elements (0.36-0.86 wt%) controlled by the activation temperatures, which are far lower than those (5.6-8.7 wt% nitrogen contents) obtained by direct pyrolysis of porous imine-linked polymer.[21] This phenomenon indicates that the nitrogen atoms tend to liberate during the one-step condensation and activation process. The nitrogen content (0.36 wt%) of MPC-750 prepared at the highest temperature of 750 °C is significantly lower than those of other samples. Also the hydrogen content gradually decreases with increasing the activation temperature in the following order: 1.01 wt% (600 °C) > 0.74 wt% (650 °C) > 0.48 wt% (700 °C) > 0.31 wt% (750 °C). These results show that the heteroatom species can be easily removed due to the decomposition/oxidation.[46] The loss of the heteroatoms is caused by the heat-treatment at high temperature, resulting in the formation and release of the nitrogen/hydrogen-containing compounds.

Table 2. CNH chemical elemental analysis of various MPCs.

Sample	N (wt%)	C (wt%)	H (wt%)
MPC-600	0.78	85.04	1.01
MPC-650	0.79	84.25	0.74
MPC-700	0.86	83.57	0.48
MPC-750	0.36	89.13	0.31

We further investigated the bonding location of N atoms in the MPCs on the basis of high-resolution N 1s XPS spectra. Quantitative elemental analysis results from the N 1s XPS spectra show the nitrogen contents in the MPCs are well in consistent with those of the chemical elemental analysis, indicating the surface of the MPCs has similar density of nitrogen functional groups as the bulk (**Table S1**). As shown in **Fig. S3**, two peaks at about 398.3 eV and 400.4 eV can be discerned from the N 1s spectra, which imply the presence of two forms of nitrogen, namely, pyridinic N and pyrrolic N.[31, 47-48] The signal for binding energy of the pyrrolic N is much higher than that of the pyridine N, showing the higher concentration of the pyrrolic N in these nitrogen-containing carbons. The nitrogen-containing groups in porous carbons are expected to act as Lewis basic sites, efficiently active for binding acidic CO_2 molecules *via* the acid-base interaction and thus improving the CO_2 uptakes.[49]

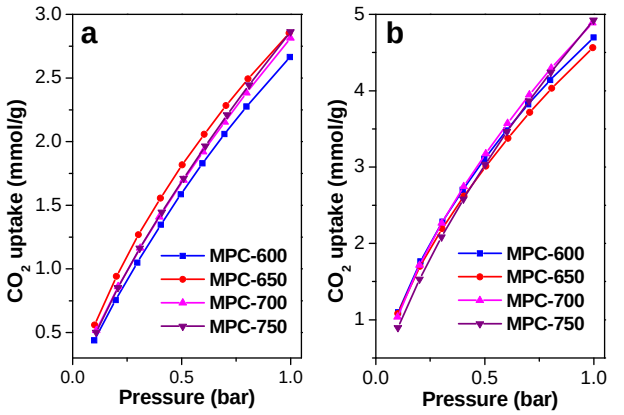

Fig. 7 CO_2 adsorption isotherms for various MPCs at 25 °C (a) and 0 °C (b), respectively.

Due to the combination of high microporosity in the range of sub-nanosize and basic nitrogen functional groups, the resulting MPCs are expected to have great potential as the physisorbents for CO_2 capture and separation.[26] The CO_2 adsorption isotherms of these MPCs collected at 25 and 0 °C, respectively are shown in **Fig. 7**. The desorption isotherms are almost consistent with the adsorption isotherms, and only a small hysteresis is formed (**Fig. S4-S11**). It shows that the capture of CO_2 by these MPCs is fully reversible. The adsorption uptakes of CO_2 at 1 bar are indicated in **Table 3**. At ambient pressure and 0 °C, MPC-600 and MPC-650 demonstrate good CO_2 uptakes of 102.2-105.2 mL/g (4.56-4.70 mmol/g) because of their large micropore surface areas (1391-1422 m^2/g), micropore volumes (0.61-0.62 cm^3/g), and narrow micropore size distribution (1.0-1.1 nm). The CO_2 uptakes (0 ^oC) increase to 109.5-110.3 mL (4.89-4.92 mmol/g) for MPC-700 and MPC-750 prepared at higher temperature, 700 and 750 °C respectively. This increase is due to not only the higher surface areas and micropore volumes, but also the narrower micropore size distributions (0.7-0.8 nm) of MPC-700 and MPC-750 compared to MPC-600 and MPC-650 samples. In the previous report, all polymer-derived activated carbons prepared at high temperatures of over 700 °C possess lower CO_2 uptakes than present MPCs (4.89-4.92 mmol/g) obtained by one-step condensation and activation of diamine and dialdehyde in the presence of KOH at 700 and 750 °C. In comparison with our results with the previous data, it can be concluded that the pore size is more important to increase gas adsorption capacities of the MPCs than the surface area and pore volume. The MPCs prepared over 700 °C possess narrow micropore sizes of 0.7-0.8 nm that thus can increase the interaction of CO_2 molecules and carbon and thus significantly improve adsorption selectivity of CO_2 over N_2. Furthermore, as shown in Fig. 7 and Table 3, the CO_2 uptakes of these MPCs at ambient temperature diminish to 2.67-2.81 mmol/g (59.6-63.8 mL). Because of an exothermic process of CO_2 physisorption, the amounts of CO_2 adsorbed decrease with increasing the environmental temperature.

Table 3. CO_2 uptakes of various MPCs at 1 bar, and 0 °C or 25 °C.

Sample	CO_2 uptake at 0 °C	CO_2 uptake at 25 °C
	mL/g (mmol/g)	mL/g (mmol/g)
MPC-600	105.2 (4.70)	59.6 (2.67)
MPC-650	102.2 (4.56)	63.8 (2.85)
MPC-700	109.5 (4.89)	63.0 (2.81)
MPC-750	110.3 (4.92)	64.1 (2.86)

To determine the strength of the interaction between the CO_2 molecules and carbon surface, the isosteric heat of adsorption (Q_{st}) for the MPCs was calculated from CO_2 adsorption isotherms measured at two temperatures (0 and 25 °C) based on the Clausius-Clapeyron equation. The calculated Q_{st} values as a function of the CO_2 uptake for the MPCs are shown in Fig. 8. The initial Q_{st} values for all MPCs lie in the range of 18-33 kJ/mol at low surface coverage, which are comparable to or higher than those reported for the previously reported activated carbons, MOFs, and covalent organic frameworks.[21, 50-53] The high Q_{st} values indicate that the MPCs strongly interact with the CO_2 molecules. It is worth noting that the initial Q_{st} values at low CO_2 uptake for the MPCs prepared at 600-700 °C are evidently higher than that for MPC-750, possibly because MPC-750 has the lowest density of nitrogen functional groups among these porous carbons. This result implies that the surface nitrogen functional groups play very important roles in the initial interaction between CO_2 molecules and carbon surface. The Q_{st} values for MPC-600 and MPC-650 significantly decrease to about 21-22 kJ/mol when the adsorbing amount of CO_2 is 3.0 mmol/g, showing that two CO_2 adsorption mechanisms coexist in these two MPCs; CO_2 molecules are adsorbed onto both the nitrogen functional groups and the non-doped porous carbon surface. Among these MPCs MPC-700 has the highest of ~28 kJ/mol at higher coverage (3.0 mmol/g), which are superior to biomass-derived porous carbons (22 kJ/mol at 0.7 mmol/g)[26] and porous polyamine (18 kJ/mol at 2.2 mmol/g),[54] since MPC-700 is characterized by both surface nitrogen functional groups and excellent textures. Sample MPC-750 which has the lowest nitrogen content and highest CO_2 uptake value, has the lowest of 16 kJ/mol at high coverage. These results imply that the nitrogen functional groups dominate the interactions between the CO_2 molecules and carbon surface at higher coverage. However for those porous carbons with lower nitrogen contents, both nitrogen functional groups and textural properties (i.e., pore size and surface area) influence the interaction of the CO_2 molecules and carbon surface. All these data above show the importance of introducing basic nitrogen functional groups and controlling the textural properties of microporous carbons in improving CO_2 uptake capacities.

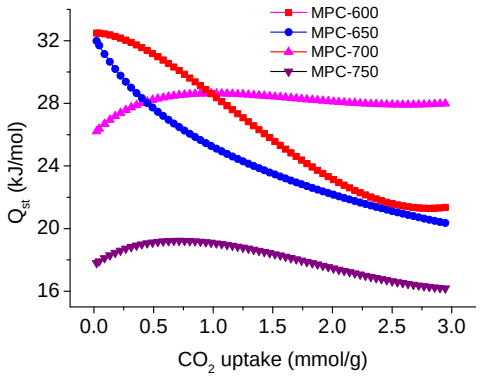

Fig. 8 Isosteric heat of CO_2 adsorption (Q_{st}) for the MPCs as a function of CO_2 uptake.

We also investigated the recycle-use ability of the MPCs as CO_2 sorbents by performing the adsorption-desorption cycle for four times at 25 °C, and the observed CO_2 adsorption capacities of MPC-750 are variable among 2.72-2.86 mmol/g at ambient pressure, implying the MPCs can be regenerated and reused without any evident loss of the adsorption capacity. Moreover the MPCs present here show comparable or higher uptakes compared to most of the previously reported porous polymers and carbons as solid adsorbents for CO_2 adsorption. For example, the doping of MgO and S-CaO-MgO in porous carbons without activation only resulted in very low CO_2 uptake of 0.28 mmol/g.[3] At 25 °C and 1 bar, activated graphite fibers, olive stone-based carbons, nitrogen-incorporated hierarchical porous carbons, and nitrogen-incorporated resin-based carbons showed poor CO_2 uptakes of 1.3, 2.0, 2.2, and 2.5 mmol/g, respectively,[55-58] far lower than our values. The CO_2 adsorption capacities of our MPCs also outperform the conjugated microporous polymer (1.45 mmol/g at 25 °C and 1 bar),[14] nanoporous melamine resin sponges (1.6 mmol/g at 0 °C),[59] and resin-based carbons (1.86 mmol/g at 25 °C).[60] At 1 bar, it can be found that the CO_2 uptake of MPC-750 is also evidently higher than those of various activated nanostructured carbons, such as widely used activated carbons (~2 mmol/g at 25 °C),[61] hard-templated CMK-3 (2.2 mmol/g at 25 °C), and CMK-8 (2.1 mmol/g at 25 °C).[22] Moreover, MPC-750 has similar CO_2 adsorption capacity to recently reported nitrogen-containing carbon framework (4.9 mmol/g at 0 °C and 1 bar) obtained by self-assembly of poly(benzoxazine-co-resol)[10] and triptycene-derived benzimidazole-linked polymers (5.1 mmol/g at 0 °C and 1 bar).[12] Thus it can be believed that the present one-step condensation and activation strategy is efficient for preparing porous carbon adsorbents for CO_2 capture with good capacity.

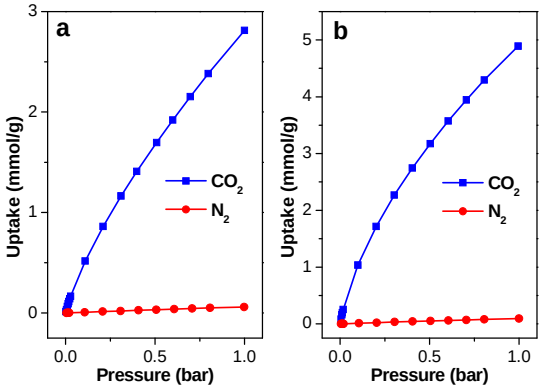

Fig. 9 CO_2 and N_2 adsorption isotherms for MPC-700 at 25 °C (a) and 0 °C (b), respectively.

Besides large CO_2 adsorption capacities toward practical applications, the MPCs should show a high adsorption ratio for CO_2 over N_2. Thus we compare the CO_2 and N_2 adsorption capacities of MPC-700 at 1 bar, and 25 and 0 °C, respectively. As presented in **Fig. 9**, the amount of CO_2 adsorbed is much higher than that for N_2 at 1 bar. At 1 bar and 25 °C, the amount of adsorbed N_2 (0.06 mmol/g) is only 2.1 % that of adsorbed CO_2 (2.81 mmol/g). With decreasing the adsorption temperature from 25 to 0 °C, the amount of adsorbed N_2 increases to 0.095 mmol/g, 1.94% that of adsorbed CO_2 (4.89 mmol/g). Therefore MPC-700 prefers to adsorb CO_2, especially at low temperatures. The calculated CO_2/N_2 adsorption ratio on MPC-700 at 1 bar is about 47 and 52 at 25 °C and 0 °C, respectively. To our knowledge, the CO_2/N_2 adsorption ratio of MPC-700 is by far the highest among various known micro-/mesoporous carbon materials under similar testing conditions. As shown in Table 4, the CO_2/N_2 adsorption ratios of our samples are far higher than those reported in the previous literatures. For example, the activated porous carbons, prepared by KOH activation of polyimine, polypyrrole, and biomass-based chars, exhibited similar CO_2/N_2 adsorption ratios of 5-9.8 at 1 bar.[21, 26, 29, 45] Kim and co-workers reported the chemical activation of graphene-modified polyaniline or polypyrrole with KOH, and the resulting graphene-based porous carbons showed that the CO_2/N_2 adsorption ratio at 1 bar and 25 °C is 9 and 17, respectively.[30-31] Direct pyrolysis of porous organic polymers/resins resulted in various porous carbons with different CO_2/N_2 adsorption ratios varying from 5 to 17.[10-11, 35, 62] Moreover, both nitrogen-doped templated and nanotube-modified porous carbons also demonstrate low CO_2/N_2 adsorption ratios of 5.8-14.[23, 63-65] Therefore it can be concluded that the CO_2/N_2 adsorption ratios of the previously reported porous carbons at ambient pressure are much lower than those of our values.

Table 4. The comparison of the CO_2/N_2 adsorption ratios for various porous carbon sorbents at 25 °C or 0 °C and 1 bar.

Sample	25 °C	0 °C	Ref.
MPC-700	**47**	**52**	**This work**
NC-800	5	5	[21]
CP-2-600	5.3	-	[29]
AS-2-600	5.4	-	[26]
PC-2	7.9	9.8	[45]
NG-7	9	-	[30]
a-NDC-6	17	-	[31]
HCM-DAH-1	17	-	[10]
NPC-650	5	6.6	[35]
RFL-500	10	-	[11]
HMT-80-900	14	-	[62]
N-TC-EMC	14	-	[63]
CEM-750	9.5	-	[64]
Com-15	5.7	5.8	[23]
CN-950	3.9	-	[65]

Because the flue gases from fossil fuel-fired power plants are composed of 70% N_2 and 15% CO_2, we also calculate the initial adsorption selectivity of CO_2/N_2 of our samples based on the initial slopes of the CO_2 and N_2 adsorption isotherms at low pressure range (**Fig. S12-S13**). As shown in **Table 5**, the calculated adsorption selectivity for CO_2 over N_2 of MPC-700 is as high as 91 and 119 at 25 and 0 °C, respectively. These initial selectivities are significantly superior to those previously reported values for various porous CO_2 sorbents. The initial selectivities for porous carbons derived from porous imine-linked polymer (12.5-23.4),[21, 35] and fungi-based porous carbons (18.5-27.3) at 25 or 0 °C are evidently poorer than those of present MPC-700.[45] Moreover these initial selectivities also surpass the triptycene-derived benzimidazole-linked polymers (39-70),[12, 66] (benzoxazine-co-resol)-based porous carbons (27.8),[10] bio-MOF-11 (81),[67] carbon nanotube/graphene modified porous carbons (17.9-34),[23, 30-31] and porous carbon templated by IBN9 (27).[68] It can be believed that MPC-700 has very high CO_2/N_2 adsorption ratio and initial absorption selectivity ascribed to its optimum micropore size (0.7 nm) as well as high micropore volume and some basic nitrogen functional groups. All these above results imply that the MPCs are potential selective sorbents for CO_2 separation from N_2, highly advantageous for practical applications.

Table 5. The comparison of the initial adsorption selectivity of CO_2 over N_2 for various porous materials calculated based on the initial slopes of the CO_2 and N_2 adsorption isotherms at 25 °C and 0 °C, respectively.

Sample	25 °C	0 °C	Ref.
MPC-700	**81**	**119**	**This work**
NC-800	-	21	[21]
NPC-650	12.5	23.4	[35]
PC-2	18.5	27.3	[45]
BILPs	39	63	[12]
BILP-1	-	70	[66]
HCM-DAH-1	27.8	-	[10]
Bio-MOF-1	-	81	[67]
Com-15	19.8	32.6	[23]
a-NDC-6	34	-	[31]
NG-7	17.9	-	[30]
IBN9-NC1-A	27	-	[68]

Conclusions

Summarizing, we have developed an efficient one-step

condensation and activation strategy to synthesize a series of microporous carbons (MPCs) using commercial available terephthalaldehyde and *m*-phenylenediamine as carbon sources. During the physical mixing of carbon sources and KOH by grinding, the aldehyde and amine groups could partially condense to form the imine bonds. Upon heat-treatment (600-750 °C), the unreacted amine and aldehyde groups further reacted *via* condensation, and then the in-situ resulting polymer was activated by KOH to form novel MPCs. These MPCs particles possess many large smooth voids with pore size of over 10 μm, and possess high surface areas of up to ~1881 m^2/g, large pore volumes of up to 0.85 cm^3/g, narrow micropore size distributions (0.7-1.1 nm), small amounts of nitrogen functional groups (0.36-0.86 %), and major fraction of porosity in the micropore range, depending on the activation temperatures (600-750 °C). It is worth noting that the samples (MPC-700 and MPC-750) prepared at high temperatures demonstrate smaller micropore systems (0.7-0.8 nm) than those (MPC-600 and MPC-650) synthesized at relatively mild conditions.

Because of well-defined micropore size (0.7-1.1 nm) and some basic nitrogen functional groups, these MPCs demonstrate good CO_2 uptakes at ambient pressure. The high-temperature activated samples have higher CO_2 uptakes than the low-temperature activated ones, because the former have an optimized micropore size (0.7-0.8 nm), highly advantageous for CO_2 adsorption. MPC-750 prepared at 700 °C has the best ability to capture CO_2 of up to 2.82 mmol/g and 4.92 mmol/g at 25 and 0 °C, respectively which are among the highest values reported for porous carbons for CO_2 capture. Moreover the MPCs also have extremely high CO_2/N_2 adsorption ratio of up to 47 (25 °C) and 52 (0 °C) at 1 bar and initial adsorption selectivity of CO_2/N_2 (81 at 25 °C and 119 at 0 °C), which are the highest reported for porous carbon-based CO_2 sorbents. Therefore these novel MPCs are potentially useful for highly selective CO_2 capture from the flue gases of power plants burning fossil fuels. Further application of these novel MPCs with optimal micropore sizes as electrodes is currently being investigated.

Acknowledgements

J. W. thanks the One Hundred Talent Plan of Chinese Academy of Sciences and National Natural Science Foundation of China (Grant No. 21307145) for the financial support. The authors are highly thankful to Dr. David Morgan in Department of Chemistry, Cardiff University for performing the XPS measurements.

Notes and references

State Key Laboratory of High Performance Ceramics and Superfine Microstructure, Shanghai Institute of Ceramics, Chinese Academy of Science, Shanghai 200050, P. R. China. Email: Jiacheng.wang@mail.sic.ac.cn; qianliu@sunm.shcnc.ac.cn; Tel: 0086-21-52412612. Fax: 0086-21-52413122

† Electronic Supplementary Information (ESI) available: Fig. S1-13 and Table S1. See DOI: 10.1039/b000000x/

1. H.-W. Häring and C. Ahner, Industrial Gases Processing, Wiley-VCH, Weinheim, 2008.
2. J. Liu, P. K. Thallapally, B. P. McGrail, D. R. Brown and J. Liu, *Chem. Soc. Rev.*, 2012, **41**, 2308.
3. Z. Yong, V. G. Mata and A. E. Rodrigues, *Adsorption*, 2001, **7**, 41.
4. O. Abass A, *Energy*, 2010, **35**, 2610.
5. Q. Wang, J. Luo, Z. Zhong and A. Borgna, *Energy Environ. Sci.*, 2011, **4**, 42.
6. R. Dawson, E. Stockel, J. R. Holst, D. J. Adams and A. I. Cooper, *Energy Environ. Sci.*, 2011, **4**, 4239.
7. A. Kumar Mishra and S. Ramaprabhu, *RSC Adv.*, 2012, **2**, 1746.
8. A. K. Mishra and S. Ramaprabhu, *J. Mater. Chem.*, 2012, **22**, 3708.
9. M. R. Mello, D. Phanon, G. Q. Silveira, P. L. Llewellyn and C. M. Ronconi, *Microporous Mesoporous Mater.*, 2011, **143**, 174.
10. G.-P. Hao, W.-C. Li, D. Qian, G.-H. Wang, W.-P. Zhang, T. Zhang, A.-Q. Wang, F. Schueth, H.-J. Bongard and A.-H. Lu, *J. Am. Chem. Soc.*, 2011, **133**, 11378.
11. G.-P. Hao, W.-C. Li, D. Qian and A.-H. Lu, *Adv. Mater.*, 2010, **22**, 853.
12. M. G. Rabbani, T. E. Reich, R. M. Kassab, K. T. Jackson and H. M. El-Kaderi, *Chem. Commun.*, 2012, **48**, 1141.
13. L. Liu, Q.-F. Deng, T.-Y. Ma, X.-Z. Lin, X.-X. Hou, Y.-P. Liu and Z.-Y. Yuan, *J. Mater. Chem.*, 2011, **21**, 16001.
14. S. Ren, R. Dawson, A. Laybourn, J.-X. Jiang, Y. Khimyak, D. J. Adams and A. I. Cooper, *Polym. Chem.*, 2012, **3**, 928.
15. J. C. Wang, X. F. Yu, Y. X. Li and Q. Liu, *J. Phys. Chem. C*, 2007, **111**, 18073.
16. J. Lee, J. Kim and T. Hyeon, *Adv. Mater.*, 2006, **18**, 2073.
17. J. C. Wang, M. Oschatz, T. Biemelt, L. Borchardt, I. Senkovska, M. R. Lohe and S. Kaskel, *J. Mater. Chem.*, 2012, **22**, 23893.
18. H. Zhou, J. Wang, J. Zhuang and Q. Liu, *RSC Adv.*, 2013, **3**, 23715.
19. H. Zhou, J. Wang, J. Zhuang and Q. Liu, *Nanoscale*, 2013, **5**, 12502.
20. J. Wang, H. Zhou, J. Zhuang and Q. Liu, *Sci. Rep.*, 2013, **3**, 3252.
21. J. C. Wang, I. Senkovska, M. Oschatz, M. R. Lohe, L. Borchardt, A. Heerwig, Q. Liu and S. Kaskel, *ACS Appl. Mater. Interfaces*, 2013, **5**, 3160.
22. M. Sevilla and A. B. Fuertes, *J. Colloid Interface Sci.*, 2012, **366**, 147.
23. Y. Jin, S. C. Hawkins, C. P. Huynh and S. Su, *Energy Environ. Sci.*, 2013, **6**, 2591.
24. K. M. K. Yu, I. Curcic, J. Gabriel and S. C. E. Tsang, *ChemSusChem*, 2008, **1**, 893.
25. M. Sevilla and R. Mokaya, *J. Mater. Chem.*, 2011, **21**, 4727.
26. M. Sevilla and A. B. Fuertes, *Energy Environ. Sci.*, 2011, **4**, 1765.
27. A. S. Ello, L. K. C. de Souza, A. Trokourey and M. Jaroniec, *Microporous Mesoporous Mater.*, 2013, **180**, 280.
28. A. S. Ello, L. K. C. de Souza, A. Trokourey and M. Jaroniec, *J. CO2 Util.*
29. M. Sevilla, P. Valle-Vigón and A. B. Fuertes, *Adv. Funct. Mater.*, 2011, **21**, 2781.
30. K. C. Kemp, V. Chandra, M. Saleh and K. S. Kim, *Nanotechnology*, 2013, **24**, 235703.
31. V. Chandra, S. U. Yu, S. H. Kim, Y. S. Yoon, D. Y. Kim, A. H. Kwon, M. Meyyappan and K. S. Kim, *Chem. Commun.*, 2012, **48**, 735.
32. V. Presser, J. McDonough, S.-H. Yeon and Y. Gogotsi, *Energy Environ. Sci.*, 2011, **4**, 3059.
33. G. Yushin, R. Dash, J. Jagiello, J. E. Fischer and Y. Gogotsi, *Adv. Funct. Mater.*, 2006, **16**, 2288.
34. Y. Gogotsi, C. Portet, S. Osswald, J. M. Simmons, T. Yildirim, G. Laudisio and J. E. Fischer, *Int. J. Hydrogen Energy*, 2009, **34**, 6314.
35. J. C. Wang, I. Senkovska, M. Oschatz, M. R. Lohe, L. Borchardt, A. Heerwig, Q. Liu and S. Kaskel, *J. Mater. Chem. A*, 2013, **1**, 10951.
36. J. C. Wang, Y. Masui and M. Onaka, *Polym. Chem.*, 2012, **3**, 865.
37. F. J. Uribe-Romo, J. R. Hunt, H. Furukawa, C. Klock, M. O'Keeffe and O. M. Yaghi, *J. Am. Chem. Soc.*, 2009, **131**, 4570.
38. P. Pandey, A. P. Katsoulidis, I. Eryazici, Y. Y. Wu, M. G. Kanatzidis and S. T. Nguyen, *Chem. Mater.*, 2010, **22**, 4974.
39. J. C. Wang, Y. Masui and M. Onaka, *Eur. J. Org. Chem.*, 2010, **2010**, 1763.
40. S.-S. Kim, J. Shah and T. J. Pinnavaia, *Chem. Mater.*, 2003, **15**, 1664.
41. R. E. Morris and P. S. Wheatley, *Angew. Chem. Int. Ed.*, 2008, **47**, 4966.
42. J. C. Wang and S. Kaskel, *J. Mater. Chem.*, 2012, **22**, 23710.
43. D. Lozano-Castello, J. M. Calo, D. Cazorla-Amoros and A. Linares-Solano, *Carbon*, 2007, **45**, 2529.
44. T. Otowa, R. Tanibata and M. Itoh, *Gas Sep. Purif.*, 1993, **7**, 241.

45. J. C. Wang, A. Heerwig, M. R. Lohe, M. Oschatz, L. Borchardt and S. Kaskel, *J. Mater. Chem.*, 2012, **22**, 13911.
46. J. C. Wang and Q. Liu, *J. Phys. Chem. C*, 2007, **111**, 7266.
47. G. Greczynski, N. Johansson, M. Logdlund, L. A. A. Pettersson, W. R. Salaneck, L. E. Horsburgh, A. P. Monkman, D. A. dos Santos and J. L. Bredas, *J. Chem. Phys.*, 2001, **114**, 4243.
48. M. R. Cohen and R. P. Merrill, *Surf. Sci.*, 1991, **245**, 1.
49. M. D. Soutullo, C. I. Odom, B. F. Wicker, C. N. Henderson, A. C. Stenson and J. H. Davis, *Chem. Mater.*, 2007, **19**, 3581.
50. B. Guo, L. Chang and K. Xie, *J. Nat. Gas Chem.*, 2006, **15**, 223.
51. A. Phan, C. J. Doonan, F. J. Uribe-Romo, C. B. Knobler, M. O'Keeffe and O. M. Yaghi, *Acc. Chem. Res.*, 2009, **43**, 58.
52. R. Banerjee, A. Phan, B. Wang, C. Knobler, H. Furukawa, M. O'Keeffe and O. M. Yaghi, *Science*, 2008, **319**, 939.
53. R. V. Siriwardane, M. S. Shen, E. P. Fisher and J. A. Poston, *Energy Fuels*, 2001, **15**, 279.
54. H.-B. Wang, P. G. Jessop and G. Liu, *ACS Macro Lett.*, 2012, **1**, 944.
55. M. G. Plaza, C. Pevida, B. Arias, J. Fermoso, M. D. Casal, C. F. Martin, F. Rubiera and J. J. Pis, *Fuel*, 2009, **88**, 2442.
56. L.-Y. Meng and S.-J. Park, *J. Colloid Interface Sci.*, 2010, **352**, 498.
57. C. Pevida, T. C. Drage and C. E. Snape, *Carbon*, 2008, **46**, 1464.
58. M. C. Gutierrez, D. Carriazo, C. O. Ania, J. B. Parra, M. L. Ferrer and F. del Monte, *Energy Environ. Sci.*, 2011, **4**, 3535.
59. A. Wilke and J. Weber, *J. Mater. Chem.*, 2011, **21**, 5226.
60. T. C. Drage, A. Arenillas, K. M. Smith, C. Pevida, S. Piippo and C. E. Snape, *Fuel*, 2007, **86**, 22.
61. S. Himeno, T. Komatsu and S. Fujita, *J. Chem. Eng. Data*, 2005, **50**, 369.
62. L. Liu, Q.-F. Deng, X.-X. Hou and Z.-Y. Yuan, *J. Mater. Chem.*, 2012, **22**, 15540.
63. L. Wang and R. T. Yang, *J. Phys. Chem. C*, 2011, **116**, 1099.
64. Y. Xia, R. Mokaya, G. S. Walker and Y. Zhu, *Adv. Energy Mater.*, 2011, **1**, 678.
65. X. Ma, M. Cao and C. Hu, *J. Mater. Chem. A*, 2013, **1**, 913.
66. M. G. Rabbani and H. M. El-Kaderi, *Chem. Mater.*, 2011, **23**, 1650.
67. J. An and N. L. Rosi, *J. Am. Chem. Soc.*, 2010, **132**, 5578.
68. Y. Zhao, L. Zhao, K. X. Yao, Y. Yang, Q. Zhang and Y. Han, *J. Mater. Chem.*, 2012, **22**, 19726.